Exp Brain Res (2003) 152:211–220
DOI 10.1007/s00221-003-1540-3

RESEARCH ARTICLE

David W. Franklin · Theodore E. Milner

Adaptive control of stiffness to stabilize hand position with large loads

Received: 7 March 2002 / Accepted: 20 May 2003 / Published online: 5 July 2003

Abstract The goal of this work was to investigate stability in relation to the magnitude and direction of forces applied by the hand. The endpoint stiffness and joint stiffness of the arm were measured during a postural task in which subjects exerted up to 30% maximum voluntary force in each of four directions while controlling the position of the hand. All four coefficients of the joint stiffness matrix were found to vary linearly with both elbow and shoulder torque. This contrasts with the results of a previous study, which employed a force control task and concluded that the joint stiffness coefficients varied linearly with either shoulder or elbow torque but not both. Joint stiffness was transformed into endpoint stiffness to compare the effect on stability as endpoint force increased. When the joint stiffness coefficients were modeled as varying with the net torque at only one joint, as in the previous study, we found that hand position became unstable if endpoint force exceeded about 22 N in a specific direction. This did not occur when the joint stiffness coefficients were modeled as varying with the net torque at both joints, as in the present study. Rather, hand position became increasingly more stable as endpoint force increased for all directions of applied force. Our analysis suggests that co-contraction of biarticular muscles was primarily responsible for the increased stability. This clearly demonstrates how the central nervous system can selectively adapt the impedance of the arm in a specific direction to stabilize hand position when the force applied by the hand has a destabilizing effect in that direction.

D. W. Franklin (✉) · T. E. Milner
School of Kinesiology,
Simon Fraser University,
Burnaby, BC V5A 1S6, Canada
e-mail: dfrank@atr.co.jp
Tel.: +81-774-951082
Fax: +81-774-952647

D. W. Franklin
ATR Computational Neuroscience Laboratories,
619–0288 Kyoto, Japan

Keywords Impedance control · Position control · Posture · Instability · Biarticular muscles

Introduction

Most of the activities performed by humans involve interacting with objects in the environment. In many of these tasks, the object applies variable forces to the hand. The mechanical impedance at the point of interaction governs the resulting motion. In particular, any external disturbance is resisted by the mechanical impedance of the arm. The ability of the central nervous system to adapt the mechanical impedance of the arm to different environmental constraints and conditions may have a significant bearing on how successfully the task can be performed.

The mechanical impedance of the arm can be modeled as comprising inertia, damping, and stiffness. The inertia of the arm changes systematically with variations in the joint angles of the arm. This can be achieved by changing the hand location in the workspace or by utilizing redundant degrees-of-freedom of the arm (Hogan 1985). Such configuration-dependent changes in inertia are paralleled by changes in stiffness (Mussa-Ivaldi et al. 1985; Flash and Mussa-Ivaldi 1990) and damping (Dolan et al. 1993; Tsuji et al. 1995). For example, the stiffness tends to increase in the direction from the shoulder to the hand and decrease in the orthogonal direction as the elbow is extended (Milner 2002b). However, unlike inertia, stiffness also depends strongly on muscle activation.

Joint stiffness has been extensively studied for joints in isolation. A number of studies have shown that joint stiffness increases linearly with joint torque under quasi-isometric conditions (Cannon and Zahalak 1982; Hunter and Kearney 1982). Recently, Gomi and Osu (1998) demonstrated that this is also the case when torque is simultaneously varied at two joints. Transformation of the relation between joint stiffness and joint torque results in variation of endpoint stiffness with the magnitude and

direction of the endpoint force (Gomi and Osu 1998; McIntyre et al. 1996; Perreault et al. 2001).

The relation between joint stiffness and joint torque is not invariant. For example, stiffness is modified in an adaptive fashion to compensate for load stability (Akazawa et al. 1983; De Serres and Milner 1991; Milner 2002a). This is achieved by co-contraction of antagonistic muscles. It has also been shown that joint stiffness is larger during position control than during force control (Akazawa et al. 1983; Doemges and Rack 1992a; Doemges and Rack 1992b) due both to increased co-contraction (Buchanan and Lloyd 1995) and reflex gain. Comparable tasks involving coordination of several joints have not yet been investigated. The magnitude of the endpoint stiffness should be similarly affected in analogous multi-joint tasks, but there could also be changes in its directional characteristics, which cannot be inferred from single joint studies.

Several studies have reported that size but not orientation or shape of the endpoint stiffness can be modified (Dolan et al. 1993; Flash and Mussa-Ivaldi 1990; Mussa-Ivaldi et al. 1985). However, a transient directional change in the endpoint stiffness was reported during a ball catching task (Lacquaniti et al. 1993). Furthermore, Gomi and Osu (1998) have shown that during controlled co-contraction subjects did exhibit some rotation of the endpoint stiffness.

Hogan (1985) suggested that humans may be able to control both the magnitude and directional characteristics of endpoint stiffness by the coordinated co-contraction of uniarticular and biarticular muscles, providing the ability to adapt the endpoint stiffness to environmental demands without changing limb posture. Recently, this was shown during arm movements by examining the adaptation to a destabilizing force field (Burdet et al. 2001). In contrast, studies examining the controllability of the endpoint stiffness during isometric tasks suggest that control of endpoint stiffness geometry is very limited (Gomi and Osu 1998; Perreault et al. 2002). The present study was undertaken to investigate how endpoint stiffness geometry would be adapted in a postural task where such adaptation was necessary for successful performance of the task. To that end, the endpoint stiffness of six subjects was measured during a position control task in which the applied endpoint force magnitude and direction were varied.

Materials and methods

Six subjects (three male and three female), ranging between 21 and 42 years of age, participated in this study. All subjects gave informed consent to the procedures, which had been previously approved by the university research ethics committee. Subjects were seated in a chair with the trunk restrained by a harness that limited movement of the subject's right arm to the shoulder and elbow joints. The subject's right hand was held in a neutral wrist position by a cast made of thermoplastic splinting material bolted to the handle of a robot manipulandum (Fig. 1). The custom-fitted cast prevented movement at the wrist joint and provided a rigid coupling between the manipulandum and the arm. The upper arm was supported in the horizontal plane, level with the right shoulder, using a sling tethered approximately 1.5 m above the subject.

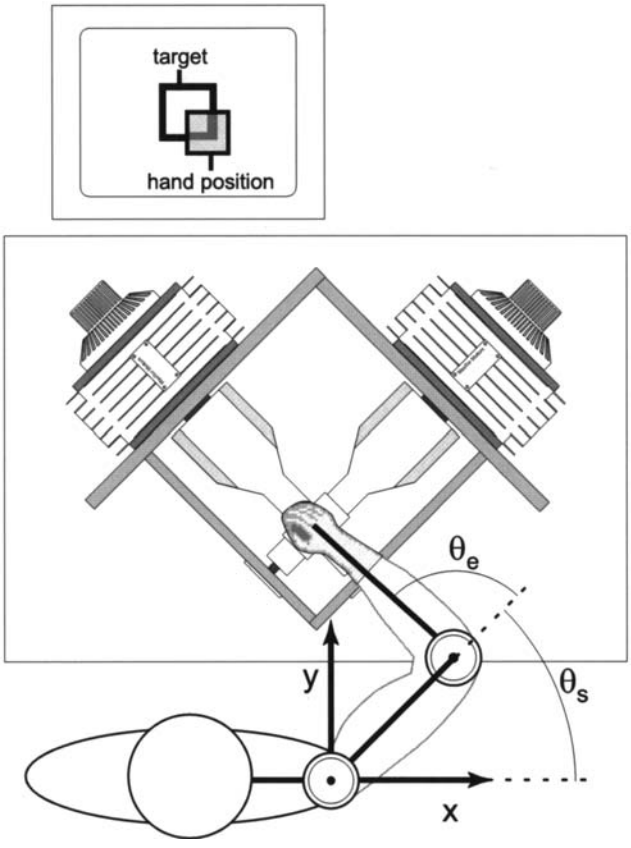

Fig. 1 The manipulandum used for estimating arm stiffness. The subject's arm was linked to the joystick by means of a splint bolted to the top of the joystick directly above the force transducer. The end of the joystick moves on a spherical surface which is approximately horizontal for small movements. Force was applied to the hand by torque motors linked to the joystick. Visual feedback of hand and target position was presented to the subject on the monitor

Apparatus

Measurements were made with a two degree-of-freedom robot manipulandum, configured so that the end effector moved along the surface of a sphere. The robot comprised two axial air gap DC servomotors (Mavilor Motors MT, Barcelona, Spain) linked by means of a gimbal (Adelstein 1989). A joystick attached to the gimbal allowed the subject to interact with the robot. The distance from the center of the gimbal to the point of interaction was 0.265 m.

A six-axis force-torque sensor (ATI FT 3175, resolution 0.1 N) at the end of the joystick measured the forces applied by the subject. The motor shaft angles were measured with brushless resolvers (MICRON No. 11) and digitized by 16 bit resolver to digital convertors (CSI 168 4800, resolution: 0.005°). Velocity and force signals were acquired at 1000 Hz with a 16-bit data acquisition card (AT-MIO-16X, National Instruments, Austin, Tex., USA). An analog control signal specifying the torque for each motor was updated at 1000 Hz and sent to a PWM current amplifier (Glentek, El Segundo, Calif., USA) that powered the torque motor. Joystick and target positions were displayed on the computer screen and updated at 20 Hz. Although an attempt was made to record EMG from relevant arm muscles, electrical noise

Table 1 Maximum voluntary force (N)

Subject	Force direction			
	45°	135°	225°	315°
A	141	284	162	268
B	136	259	154	212
C	98	204	152	179
D	86	189	127	160
E	93	172	142	135
F	50	39	69	51

generated by the torque motors interfered with the EMG signal to the extent that no corroboration of the results using EMG was possible.

Protocol

The endpoint stiffness of the arm was measured in a flexed posture with the shoulder at 45° of forward flexion and the elbow joint flexed by 90°. In addition to the shoulder and elbow angles, the distances from the center of rotation of the elbow to the center of the joystick and between the centers of rotation of the shoulder and elbow were measured for each subject. The subject opposed forces produced by the robot directed at 45°, 135°, 225°, and 315° to the subject's frontal plane. Maximum isometric voluntary contractions (MVC) were first recorded for each subject in each of these four directions with the joystick clamped at the central position. The force levels used in subsequent experiments were percentages [0% (relaxed), 7.5%, 15%, 22.5% and 30%] of the MVC in each direction. The MVCs for each subject are listed in Table 1.

The subject was instructed to control the position of the joystick. The robot generated a force, which the subject was required to oppose to remain at the target position. This differs from previous studies (Gomi and Osu 1998; Perreault et al. 2001) which employed a force control task where the subject's hand was stabilized by servo-control while the subject produced a target force. In the present study, subjects were required to hold the joystick in a 4 mm square target window. Once the target position had been maintained for a randomly variable period of 1–3 s, the hand was displaced. The display of joystick position was frozen during the displacement.

To estimate the stiffness, perturbations were applied in eight directions, uniformly distributed over 360°. A pulse-step force perturbation was used to move the arm to a new position (Fig. 2). The resulting movement was similar to a ramp and hold displacement. The size of the force pulse was varied, depending on the displacement direction and experimental condition, to produce a consistent displacement of approximately 10 mm. The displacement was small enough that the hand essentially remained in the horizontal plane (the deviation from horizontal was less than 0.2 mm). Forty-eight trials were recorded for each condition, i.e., six for each displacement direction. Subjects were instructed not to react voluntarily to the displacement. The order of conditions (force direction, force level, and perturbation direction) was randomized throughout the experiment and across subjects.

Analysis

The endpoint stiffness at the hand and the joint stiffness at the elbow and shoulder were calculated from the measured change in force and displacement. Joint stiffness had previously been estimated together with inertia and damping by fitting a second-order model to the entire response (Gomi and Kawato 1997; Gomi and Osu 1998). However, an estimate of the joint stiffness, which is independent of inertia and damping, can be obtained by considering only the portion of the response where acceleration and velocity are low enough that contributions to the joint torque from inertia and damping can be neglected. This occurred at the time of peak displacement. The stiffness was estimated from the equation:

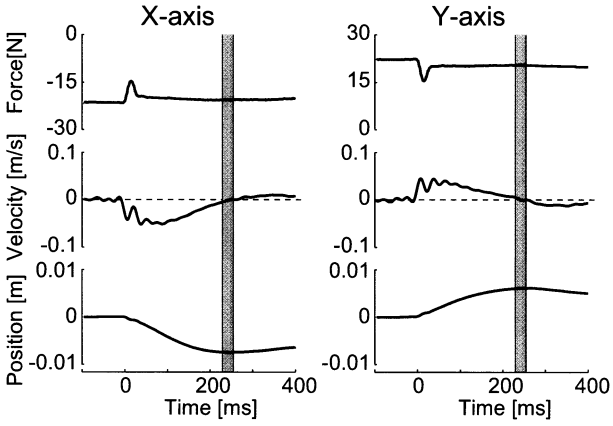

Fig. 2 Traces of force and position during a perturbation in the 315° direction. The force perturbation consisted of a pulse that displaced the hand and a bias (step) that maintained an approximately constant displacement during the measurement interval. The *shaded region* indicates the interval during which the joint and endpoint stiffness were measured. During this period the velocity was near zero

$$\begin{bmatrix} d\tau_s \\ d\tau_e \end{bmatrix} = \begin{bmatrix} R_{ss} & R_{se} \\ R_{es} & R_{ee} \end{bmatrix} \begin{bmatrix} dq_s \\ dq_e \end{bmatrix} \quad (1)$$

using linear regression. Joint angles, q, and torques, τ, were obtained by transforming the position and force from Cartesian space to joint space using inverse kinematics and the Jacobian transformation matrix. The mean joint angles and torques during a 320-ms interval prior to the onset of the displacement were subtracted from instantaneous values during a 26-ms interval, centered on the time of peak displacement, to obtain the differentials. During this interval, the values of acceleration and velocity were low enough that inertial and damping forces could be ignored. The components of the joint stiffness matrix for each experimental condition were then determined using least squares multiple linear regression of the data from all 48 trials. Two relations between joint stiffness and joint torque were examined, a single and a multiple linear regression model, using the data of individual subjects and the pooled data of all subjects. The univariate (single independent variable) relation [corresponding to that found by Gomi and Osu (1998)] was expressed as:

$$\begin{bmatrix} R_{ss} & R_{se} \\ R_{es} & R_{ee} \end{bmatrix} = \begin{bmatrix} m_1|\tau_s| + b_1 & m_2|\tau_e| + b_2 \\ m_3|\tau_e| + b_3 & m_4|\tau_e| + b_4 \end{bmatrix}. \quad (2)$$

The second relation, a bivariate (two dependent variables) relation, which allowed each joint stiffness coefficient to vary with both shoulder and elbow torque, was expressed as:

$$\begin{bmatrix} R_{ss} & R_{se} \\ R_{es} & R_{ee} \end{bmatrix} = \begin{bmatrix} m_{1a}|\tau_s| + m_{1b}|\tau_e| + b_1 & m_{2a}|\tau_s| + m_{2b}|\tau_e| + b_2 \\ m_{3a}|\tau_s| + m_{3b}|\tau_e| + b_3 & m_{4a}|\tau_s| + m_{4b}|\tau_e| + b_4 \end{bmatrix}. \quad (3)$$

The endpoint stiffness, expressed in Cartesian coordinates, was computed using the method of Mussa-Ivaldi et al. (1985). The static mean force, F, and the position vector, x, during the 320-ms interval prior to displacement were subtracted from the instantaneous values during the 26-ms interval to obtain the differentials. The stiffness matrix was estimated using multiple linear regression.

$$\begin{bmatrix} dF_x \\ dF_y \end{bmatrix} = \begin{bmatrix} K_{xx} & K_{xy} \\ K_{yx} & K_{yy} \end{bmatrix} \cdot \begin{bmatrix} dx \\ dy \end{bmatrix} \quad (4)$$

The endpoint stiffness can be represented in terms of the eigenvalues of the stiffness matrix using an ellipse, where the major and minor axes correspond to the maximum and minimum eigenvalues. Singular value decomposition of the stiffness matrix *K* was used to find the eigenvalues (Gomi and Osu 1998).

Geometric and muscle contributions to stiffness

Endpoint stiffness is represented in Eq. 5 as the sum of two coefficients, which will be referred to as endpoint muscle stiffness and geometric stiffness when represented in Cartesian space.

$$\mathbf{K} = \mathbf{J}^{-1T}\left[\mathbf{R} - \frac{\partial \mathbf{J}^T}{\partial \theta}\mathbf{F}\right]\mathbf{J}^{-1} \quad (5)$$

The endpoint muscle stiffness, which is the first coefficient on the right side of Eq. 5, arises from the change in muscle force that accompanies muscle length changes during the displacement of the arm. The geometric stiffness does not arise from muscle properties, but rather from changes in shoulder and elbow angle that affect the transformation of joint torques to endpoint force. The geometric stiffness is zero when endpoint force is zero and increases in proportion to the endpoint force. The endpoint muscle stiffness was obtained from the joint stiffness, *R*, by setting the force equal to zero. The geometric stiffness was then calculated by subtracting the endpoint muscle stiffness from the total endpoint stiffness, i.e., the term on the left-hand side of Eq. 5.

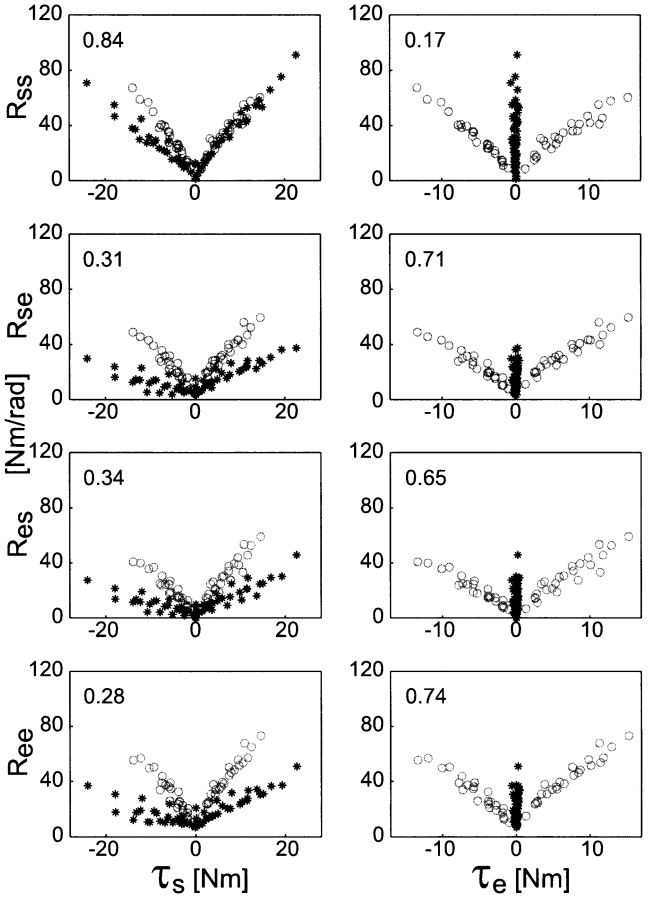

Fig. 3 Joint stiffness plotted against shoulder and elbow torque. Each coefficient of the joint stiffness matrix is plotted against both shoulder torque and elbow torque. The correlation coefficient (r^2) of each relation is shown in the *top left-hand corner of each panel*. Data from all six subjects are shown. For conditions where the elbow torque was zero, the data are represented by *black stars* whereas for conditions where the elbow torque was non-zero the data are represented by *grey circles*

Results

Position and force records used in estimating stiffness are illustrated in Fig. 2. The changes in force and displacement between the shaded region and the respective values prior to the perturbation were used in estimating stiffness. The mean latency to the center of the shaded region was 228±51 ms after perturbation onset.

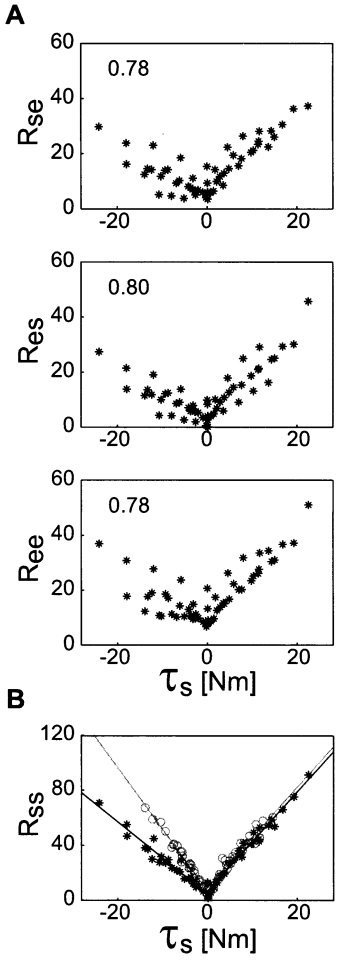

Fig. 4 **A** Elbow and cross-joint stiffness are shown in relation to shoulder torque for conditions where elbow torque was zero. Correlation coefficients for each relation are shown in the *upper left corner of each panel*. Data from all six subjects are shown. **B** Shoulder stiffness is shown in relation to elbow torque. The shoulder stiffness is plotted separately for zero elbow torque (*black stars*) and non-zero elbow torque (*grey circles*). The *light lines* represent the linear regression for zero elbow torque and the *dark lines* for non-zero elbow torque. The shoulder stiffness was higher in cases where elbow torque was non-zero for both the positive and negative shoulder torque directions. This indicates a dependence of shoulder stiffness on elbow torque

Table 2 Bivariate stiffness relation with joint torque [slopes, intercepts, 95% confidence intervals (CI), and correlation coefficients]. Each stiffness coefficient is related to both shoulder torque (τ_s) and elbow torque (τ_e)

Subject	τ_s Slope±CI	τ_e Slope±CI	Intercept±CI	Correlation coefficient
(a) R_{ss}				
A	2.77±0.50	0.94±0.63	13.39±7.01	0.91
B	2.68±0.68	1.24±0.78	11.07±7.54	0.86
C	2.76±0.62	1.19±0.71	6.81±5.29	0.89
D	3.07±1.02	0.94±1.12	5.36±7.05	0.79
E	3.22±0.97	0.74±0.98	5.47±7.03	0.81
F	4.22±0.75	1.27±0.62	2.94±1.45	0.98
All	3.03±0.23	1.14±0.30	6.55±2.01	0.90
(b) R_{se}				
A	0.73±0.33	2.24±0.42	14.55±4.61	0.92
B	0.97±0.49	2.42±0.57	8.03±5.51	0.88
C	0.72±0.53	2.90±0.61	8.74±4.50	0.90
D	1.01±0.86	2.30±0.94	8.81±5.97	0.74
E	0.96±0.69	2.53±0.70	3.50±5.01	0.85
F	1.41±1.15	3.30±0.95	4.34±2.23	0.94
All	1.02±0.19	2.53±0.25	7.05±1.67	0.86
(c) R_{es}				
A	1.03±0.54	2.08±0.68	8.65±7.54	0.81
B	0.77±0.49	2.49±0.57	7.78±5.50	0.88
C	0.85±0.45	2.78±0.52	5.75±3.88	0.92
D	1.32±0.89	1.95±0.97	4.49±6.12	0.72
E	0.76±0.41	2.26±0.42	1.23±2.99	0.93
F	1.50±0.73	2.55±0.60	2.20±1.41	0.96
All	1.12±0.20	2.37±0.26	3.88±1.78	0.84
(d) R_{ee}				
A	0.92±0.50	2.57±0.64	18.38±7.05	0.86
B	0.80±0.49	3.27±0.57	12.58±5.52	0.92
C	0.63±0.68	3.70±0.79	11.36±5.85	0.89
D	1.25±0.98	2.52±1.07	11.24±6.76	0.74
E	1.11±0.74	3.15±0.75	8.84±5.42	0.88
F	1.48±1.13	3.71±0.94	6.95±2.20	0.95
All	1.12±0.22	3.11±0.29	10.24±1.91	0.87

Joint stiffness

Each joint stiffness coefficient was plotted against elbow and shoulder joint torque to investigate the nature of the relation between joint stiffness and joint torque during position control as the applied force was varied (Fig. 3). The single joint shoulder stiffness (R_{ss}) was found to be more highly correlated with shoulder torque than elbow torque while the cross-joint and elbow stiffness coefficients (R_{se}, R_{es}, and R_{ee}) were more strongly correlated with elbow torque. However, the data suggest that a univariate relation between joint stiffness and joint torque may not be the best model. In particular, it can be seen that the elbow stiffness (R_{ee}) and cross-joint stiffness (R_{se} and R_{es}) coefficients varied between approximately 0 and 40 Nm/rad when elbow torque was zero. This indicates that elbow and cross-joint stiffness coefficients may also have co-varied with shoulder torque as the endpoint force was increased.

To test whether this occurred, linear regression was performed between stiffness and shoulder torque for trials where elbow torque was zero (Fig. 4A). High correlations were found between elbow and cross-joint stiffness coefficients and shoulder torque (0.85, 0.84, and 0.82).

The shoulder stiffness data were separated into two groups: shoulder stiffness estimates for trials where the elbow torque was approximately zero ($|\tau_e| \leq 0.8$ Nm) and shoulder stiffness estimates for trials where the elbow torque was non-zero ($|\tau_e| > 0.8$ Nm) (Fig. 4B). Differences between the two groups were examined using an ANCOVA with covariate shoulder torque for each direction of shoulder torque (positive and negative). The shoulder joint stiffness was found to be significantly larger when elbow torque was non-zero than when elbow torque was zero for both the positive (P=0.005) and negative (P<0.001) shoulder torque directions. This demonstrates that the joint stiffness varied with both elbow and shoulder torque. Multiple linear regression was then performed on the data of individual subjects and on the pooled data of all subjects using the model of Eq. 3. This was compared to the univariate model of Gomi and Osu (1998) where the shoulder stiffness coefficient (R_{ss}) varied with shoulder torque only while the other three coefficients (R_{se}, R_{es}, and R_{ee}) varied with elbow torque only (Eq. 2). The univariate model did not account for as much of the variance in the data [R^2=0.84 0.71 0.65 0.74] as the bivariate model [R^2=0.90 0.86 0.84 0.87]. Therefore, the bivariate model better describes the variation in joint stiffness during the position control task. The regression coefficients for the bivariate relation are listed in Table 2 along with the correlation coefficients.

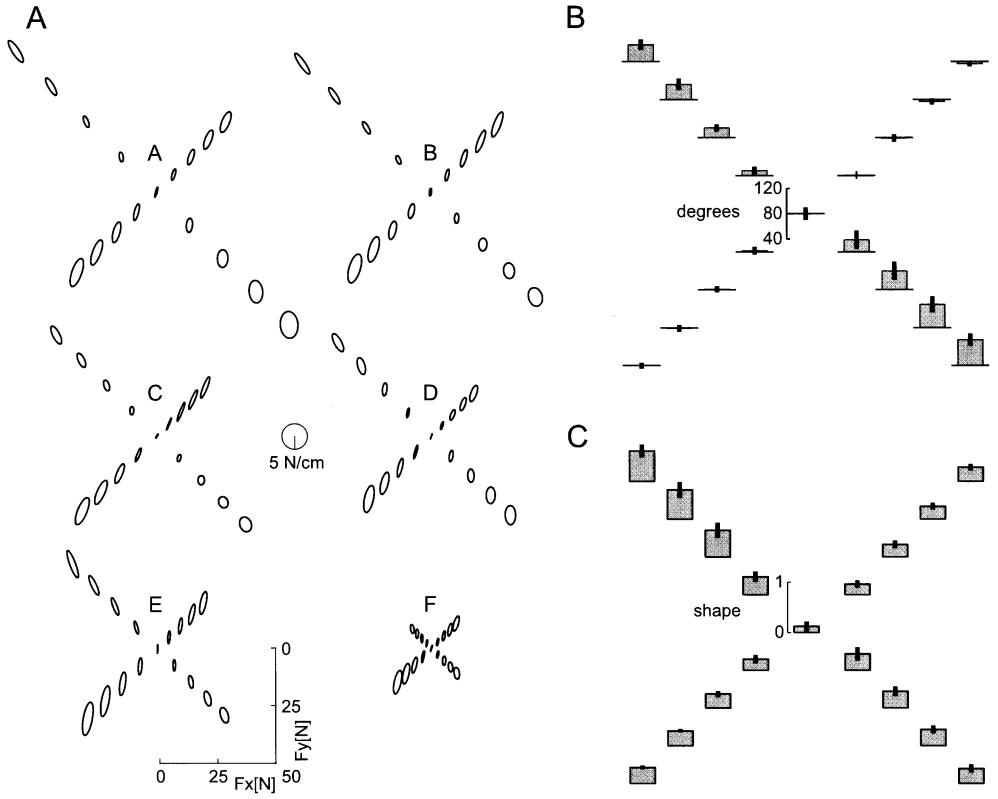

Fig. 5 **A** The endpoint stiffness ellipses of all six subjects (*A–F*) are shown for each of seventeen conditions. The central ellipse represents the stiffness with the arm relaxed. The other ellipses are organized outwards in the direction that the force was applied. The distance to the center of an ellipse from the center of the central ellipse represents the applied force as indicated by the scale at the bottom left. All ellipses are drawn to the same scale, which is indicated in the middle of the figure. **B** Orientation of the endpoint stiffness ellipse for each of the force conditions. The mean value of the six subjects (*bar*) and the standard deviation (*line*) are shown. The position of the bar indicates the condition as in **A**. **C** Mean and standard deviation of the shape of the endpoint stiffness ellipses for all conditions. Shape is expressed as a number from 0 (*straight line*) to 1 (*circle*) and calculated as in Gomi and Osu (1998)

Endpoint stiffness

The endpoint stiffness ellipses of all six subjects are plotted in Fig. 5. The ellipse geometry is based on the eigenvectors and eigenvalues obtained from the singular value decomposition of the stiffness matrices. The stiffness changed shape, size, and orientation as the endpoint force magnitude was varied. The size of the ellipse increased as larger forces were applied in each of the four directions. The shape of the endpoint stiffness also became more isotropic as endpoint force increased, particularly in the 135° force direction. The orientation of the endpoint stiffness varied depending on the direction of force. In general, this change in orientation became more prominent as the force level increased.

Endpoint muscle stiffness and geometric stiffness

The decomposition of endpoint stiffness into geometric and muscle stiffness was carried out for all force conditions investigated in this study. The endpoint muscle stiffness and total endpoint stiffness for one subject are shown in Fig. 6A along with the effect of the geometric stiffness on the maximum and minimum eigenvalues of the stiffness matrices (Fig. 6B and C).

The geometric stiffness increased with endpoint force. It produced an increase in endpoint stiffness when the applied force was in the negative*y*-direction (towards the body) and a decrease when the applied force was in the positive*y*-direction (away from the body). Geometric stiffness had a large effect on the minimum eigenvalue of the stiffness matrix (Fig. 6B), which changed by as much as 200 N/m as endpoint force increased to 100 N. In contrast, geometric stiffness had relatively little effect on the maximum eigenvalue for the force directions of this study.

We used the relation between joint stiffness and joint torque with the mean regression coefficients reported by Gomi and Osu (1998) to simulate how endpoint stiffness would vary with endpoint force in a force control task. The results are shown in Fig. 6D and E for the 135° direction. As the endpoint force increases, stiffness in the direction of the minimum eigenvalue decreases monotonically. This closely matches the behavior of the measured endpoint stiffness depicted in Fig. 10 of their paper (Gomi and Osu 1998). At a force of 22 N, the minimum eigenvalue and stiffness become negative,

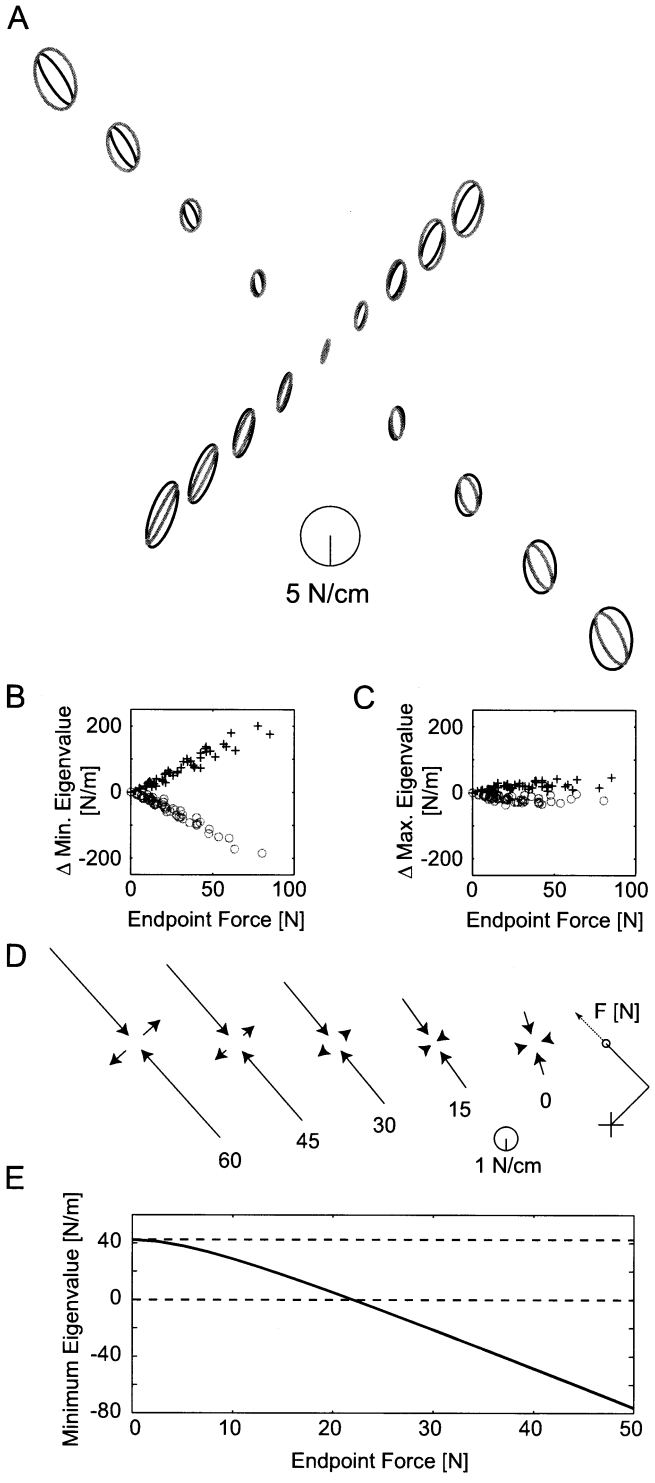

Fig. 6 **A** Endpoint stiffness and endpoint muscle stiffness shown for subject A. Endpoint muscle stiffness ellipses are represented by *thick grey lines*. Total endpoint stiffness is represented by *thin dark lines*. Layout of the plot is the same as Fig. 5. **B, C** Effect of geometric stiffness on total endpoint stiffness. Change in minimum (**B**) and maximum (**C**) eigenvalue produced by the geometric stiffness as a function of endpoint force. *Black crosses* represent conditions where the *y*-axis force is negative or towards the body. *Light circles* represent conditions where the *y*-axis force is positive or away from the body. **D** Endpoint stiffness produced by the univariate relation using the mean slope and intercepts of Gomi and Osu (1998) for the 135° force direction. The magnitude and direction of the restoring force in response to a displacement is shown by the *arrows* along the directions of the minimum and maximum eigenvalues. This minimum eigenvalue gradually decreases until the restoring force begins to assist the displacement. The arm posture and force direction are illustrated at the far right. **E** The minimum eigenvalue of the univariate relation (as in **D**) expressed as a function of endpoint force for force in the 135° direction. The minimum eigenvalue decreases monotonically and becomes negative for endpoint forces above 22 N

signifying instability parallel to the narrow axis of the stiffness ellipse. Furthermore, instability becomes greater as the applied force increases. Since the position of the hand was servo-controlled by the robot (Gomi and Osu 1998), this instability was compensated by the stiffness of the position servo. However, had the central nervous system relied on such a strategy during our position control task, subjects would not have been able to successfully perform the task.

Stability of the bivariate relation

In our position control task, the joint stiffness coefficients scaled with both elbow and shoulder torque. In light of the failure of a univariate relation to provide adequate stability at moderate to high force levels, a likely rationale for a bivariate relation would be to afford greater stability. If so, the endpoint stiffness should be greater in the direction of least stability, represented by the minimum eigenvalue of the endpoint stiffness matrix, with a bivariate relation compared to a univariate relation between stiffness and torque. To test this hypothesis, the maximum and minimum eigenvalues of the stiffness matrix, modeled with each relation, were compared for each force direction using an ANCOVA with covariate endpoint force level. The results of this comparison are shown in Fig. 7. The differences between stiffness eigenvalues for the two relations depended on the direction of applied force. Generally, the eigenvalues increase as the endpoint force increases. However, the slope depends on the direction of applied force. The minimum eigenvalues obtained with the bivariate model were larger in the 45° ($P<0.001$) and 135° ($P<0.001$) directions than those obtained with the univariate model. In the 315° force direction there was no difference between the minimum eigenvalues obtained with the two models ($P=0.464$). In the 225° force direction, the minimum eigenvalues were slightly smaller with the bivariate than the univariate model ($P<0.001$). However, in this force direction the bivariate stiffness ellipses were rotated (clockwise 28.35°) with respect to the univariate stiffness ellipses. In contrast to the univariate relation, the bivariate relation generated positive endpoint stiffness under all conditions.

The maximum eigenvalues were always positive and increased with endpoint force regardless of the direction of applied force. There was no difference between the

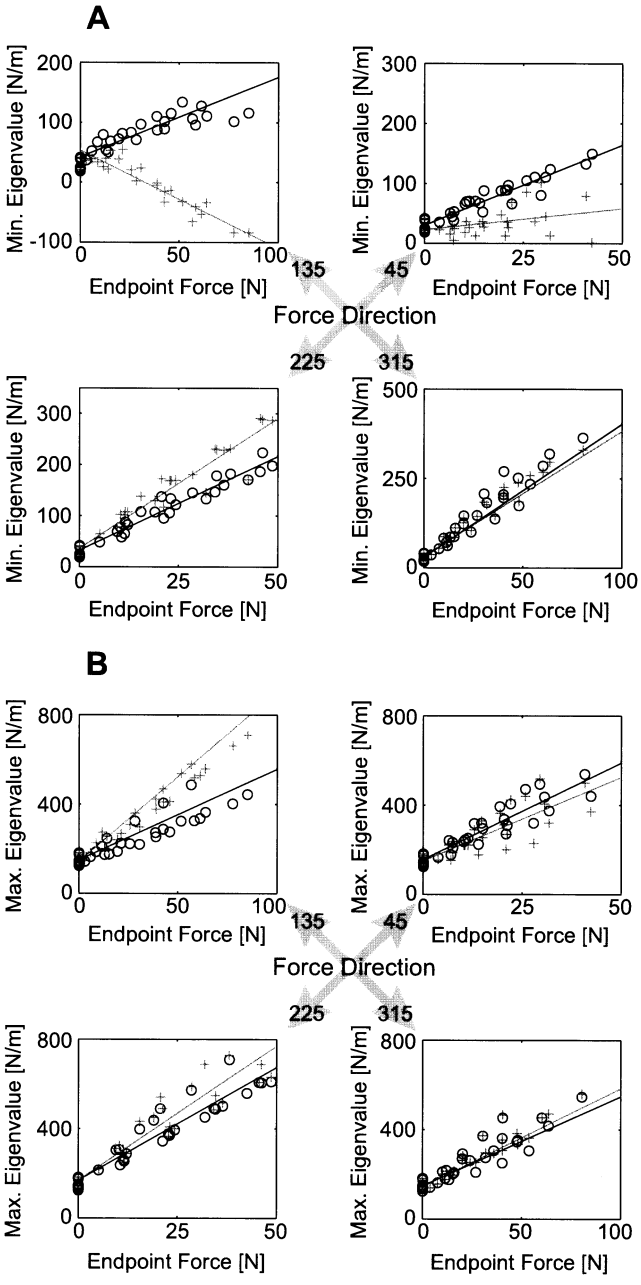

Fig. 7A, B Comparisons of minimum and maximum eigenvalues for force control and position control tasks, computed from linear regression equations. **A** Minimum eigenvalues shown as a function of endpoint force. Values for endpoint stiffness produced by a bivariate relation (corresponding to a position control task) are plotted as *dark circles* along with the best-fit line (*dark line*). Endpoint stiffness under force control was computed from a univariate relation [as in Gomi and Osu (1998)]. Eigenvalues are plotted as *light crosses* along with the best-fit line (*light line*). Each panel corresponds to the force direction indicated at the center of the figure. **B** Maximum eigenvalues as a function of endpoint force, represented as in **A**

maximum eigenvalues of the bivariate and univariate models for force directions of 45° (P=0.116) and 315° (P=0.440). The slope of maximum eigenvalue with endpoint force was slightly higher in the 225° direction (P=0.037) and lower in the 135° direction (P<0.001) for the bivariate as compared to the univariate model.

Discussion

We have shown that joint stiffness is modulated in a different manner during position control, when the central nervous system must compensate for mechanical instability, compared to force control, when position is externally stabilized (Gomi and Osu 1998; Perreault et al. 2001). We found that each coefficient of the joint stiffness matrix varied with both shoulder and elbow torque. This bivariate relation between joint stiffness and joint torque effectively increased the stiffness at the hand to ensure that posture would remain stable despite an increasing tendency toward instability due to negative geometric stiffness as applied force increased. The nature of the bivariate relation suggests that biarticular muscles played an important role in stabilizing hand position.

Comparison with previous studies

Stiffness of the relaxed arm has been measured in a number of studies (Mussa-Ivaldi et al. 1985; Tsuji et al. 1995; McIntyre et al. 1996; Gomi and Osu 1998; Perreault et al. 2001). Our results for the relaxed arm are similar to those of earlier studies. We found that both the single joint and cross-joint coefficients of the stiffness matrix fell between the maximum and minimum values previously reported for a comparable posture of the arm. In the two previous studies where endpoint force direction and magnitude were varied, a linear relation between joint stiffness and joint torque was found (Gomi and Osu 1998: Perreault et al. 2001). The investigators determined that a single regression variable, either shoulder or elbow torque, adequately explained the variance in the data. Shoulder stiffness varied with shoulder joint torque, while cross-joint and elbow stiffness varied with elbow torque. In both of these studies, subjects performed a force control task. We, on the other hand, investigated position control and found that a single regression variable could not account for as much of the variance in the data as it had in the force control task. However, a multiple linear regression model, in which each coefficient of the joint stiffness matrix varied with both elbow and shoulder torque, accounted for more of the variance in the position control data. Our analysis suggests that this difference is likely attributable to potential mechanical instability when applying force during position control.

Mechanical stability

The mechanical stability of an arm posture can be assessed from the endpoint stiffness. For planar motion, in which only two joints participate (elbow and shoulder), arm posture is stable if both eigenvalues of the endpoint

stiffness matrix are positive, i.e., the stiffness is positive in all directions, ensuring that the arm will return to its original position after a small displacement (McIntyre et al. 1996). Since the eigenvalues are generally not equal, the margin of stability is better represented by the smaller of the two eigenvalues. Therefore, our discussion will focus on how the smaller or minimum eigenvalue varies with the applied force vector.

The endpoint stiffness can be separated into a muscle and a geometric component. The geometric component can be attributed solely to the geometric transformation between joint torque and endpoint force, which necessitates that endpoint force changes whenever joint angles change. Our analysis demonstrates that the geometric stiffness can be stabilizing (increase the minimum eigenvalue) or destabilizing (reduce the minimum eigenvalue), depending on the direction of the applied force vector. Furthermore, the amount of stabilization or destabilization (change in the minimum eigenvalue) conferred by the geometric stiffness is directly proportional to the magnitude of the applied force. For those force directions in which geometric stiffness is destabilizing, the decrement in geometric stiffness with applied force must be offset by a corresponding increment in endpoint muscle stiffness for the posture of the arm to remain stable as applied force increases.

All previous studies which investigated the relation between endpoint stiffness and applied force provided the subject with some form of external stabilization. Hand position was servo-controlled in the studies of Gomi and Osu (1998) and Perreault et al. (2001), while cable tension provided stability orthogonal to the direction of the load in the study of McIntyre et al. (1996). In our case, the task was inherently unstable because the joystick behaved like an inverted pendulum with very little friction. Since the task was to control the position of the joystick while opposing an external force, the subject had to stabilize the joystick. Furthermore, the subject also had to compensate for any reduction in stability when the force direction corresponded to the direction in which geometric stiffness produced a decrement in the minimum eigenvalue. This requirement appears to be responsible for our observation that all coefficients of the joint stiffness matrix depend on both elbow and shoulder torque (which we refer to as a bivariate model). This contrasts with the results of the force control studies in which joint stiffness was adequately represented by a dependence on only elbow or shoulder torque, i.e., a univariate model.

By comparing the effect of torque variation on endpoint stiffness using bivariate and univariate models with experimentally derived parameters, we showed that the minimum eigenvalue of the endpoint stiffness derived from the bivariate model was always greater than or equal to that derived from the univariate model. The difference was most striking when the force direction corresponded to that in which the geometric stiffness reduced the minimum eigenvalue of the endpoint stiffness. In this case, the endpoint muscle stiffness resulting from the univariate model was insufficient to counteract the decrement in geometric stiffness. The minimum eigenvalue became negative when the applied force exceeded 22 N, implying that the arm would have been mechanically unstable for forces greater than 22 N.

Task dependence of joint stiffness

Joint stiffness during force control and position control has been compared in studies which isolated movement to the distal joint of the thumb (Akazawa et al. 1983) or to the flexion-extension axis of the wrist (Doemges and Rack 1992a; Doemges and Rack 1992b). Higher stiffness was reported during position control than force control due to co-contraction of agonist and antagonist muscles and/or greater stretch reflex responses. Similarly, clear differences in muscle activity were seen in the elbow joint for these two tasks (Buchanan and Lloyd 1995). Our multi-joint position control task presented the central nervous system with a higher dimensional problem than that of the single-joint studies. The central nervous system now had to solve the problem of controlling position in the face of anisotropic, force-dependent instability. The bivariate relation between joint stiffness and elbow and shoulder torque suggests that the central nervous system used selective co-contraction of the biarticular muscles to achieve stability. McIntyre et al. (1996) showed that the combined stiffness of biarticular and single-joint muscles provided more uniform endpoint stiffness than could be achieved with single-joint muscles alone. However, in their constrained position control task they were not able to demonstrate that subjects exploited the properties of biarticular muscles to adaptively control the geometry of the endpoint stiffness. In contrast, by reducing stability in one direction only, Franklin et al. (2003) found that selective activation of biarticular muscles could dramatically transform endpoint stiffness geometry. If biarticular muscles are used principally to counteract instability then they would be expected to contribute much less to endpoint stiffness in force control tasks where stability is provided by external constraints.

Indeed, this is precisely what Perreault et al. (2001) found. The slope of the relation between cross-joint stiffness and shoulder torque was considerably less than what we found and in some cases was not even significantly different from zero. Furthermore, they found that elbow stiffness did not vary at all with shoulder torque [R_{ee} vs T_s]=[−0.08] rad^{-1}. Since any change in stiffness of the biarticular muscles should have contributed to a similar change in single-joint elbow stiffness, we can infer from their results that biarticular muscle stiffness did not vary with shoulder torque. It would appear, therefore, that the dependence of cross-joint stiffness and elbow stiffness on shoulder torque, which arises from selective activation of biarticular muscles, does not occur when the arm is stabilized by external constraints.

The dependence of cross-joint stiffness and elbow stiffness on shoulder torque could result from either

increased co-contraction of the biarticular muscles or increased gain of heterogenic reflexes. The latter seems the less likely possibility. First, we already have strong evidence of selective co-contraction of biarticular muscles in another task in which the minimum eigenvalue of the endpoint stiffness was effectively reduced by a destabilizing force field (Burdet et al. 2001; Franklin et al. 2003). Second, there is no evidence that the strength of heterogenic reflexes of the elbow and shoulder vary with joint torque. Smeets and Erkelens (1991) found that the heterogenic stretch reflex response in a single joint elbow flexor was independent of shoulder torque. Furthermore, since the torque produced by even the fastest reflex responses is delayed by at least 50 ms with respect to the stimulus (Stein and Kearney 1995), high reflex gains may lead to greater instability in the form of tremor (Prochazka and Trend 1988). One other possibility is that a triggered response could have contributed to the effects seen in this study. However, when asked, subjects are able to suppress triggered reactions (Crago et al. 1976). Also, the nature of the protocol, where force direction, force level, and perturbation direction were randomized, would have involved such a large repertoire of responses that the preparation of an appropriate triggered response for each condition would have been very unlikely. Furthermore, no evidence of such a response was detected in comparing the position traces of trials recorded near the beginning of the experimental session and the end, at which point, had subjects learned triggered responses, they would have been more likely to produce them. Therefore, we conclude that the bivariate relation between joint stiffness and joint torque must be principally due to co-contraction of biarticular muscles and that this represents a difference between a position control task, such as ours, and a force control task in which position is stabilized by external constraints. This is yet another example of the ability of the central nervous system to adaptively control the mechanical impedance of the arm (Hogan 1985).

Acknowledgements This work was supported by a grant from the National Science and Engineering Research Council of Canada. DWF was also supported in part by the Telecommunications Advancement Organization of Japan. We thank Dr. M. J. Grey for his contributions as well as Drs. M. Kawato, E. Burdet, and R. Osu for related discussions.

References

Adelstein D (1989) A virtual environment system for the study of human arm tremor. PhD Dissertation, M.I.T., Cambridge, MA

Akazawa K, Milner TE, Stein RB (1983) Modulation of reflex EMG and stiffness in response to stretch of human finger muscle. J Neurophysiol 49:16–27

Buchanan TS, Lloyd DG (1995) Muscle activity is different for humans performing static tasks which require force control and position control. Neurosci Lett 194:61–64

Burdet E, Osu R, Franklin DW, Milner TE, Kawato M (2001) The central nervous system stabilizes unstable dynamics by learning optimal impedance. Nature 414:446–449

Cannon SC, Zahalak GI (1982) The mechanical behavior of active human skeletal muscle in small oscillations. J Biomech 15:111–121

Crago PE, Houk JC, Hasan Z (1976) Regulatory actions of human stretch reflex. J Neurophysiol 39:925–935

De Serres SJ, Milner TE (1991) Wrist muscle activation patterns and stiffness associated with stable and unstable mechanical loads. Exp Brain Res 86:451–458

Doemges F, Rack PM (1992a) Changes in the stretch reflex of the human first dorsal interosseous muscle during different tasks. J Physiol 447:563–573

Doemges F, Rack PM (1992b) Task-dependent changes in the response of human wrist joints to mechanical disturbance. J Physiol 447:575–585

Dolan JM, Friedman MB, Nagurka ML (1993) Dynamic and loaded impedance components in the maintenance of human arm posture. IEEE Trans Systems Man Cybern 23:698–709

Flash T, Mussa-Ivaldi F (1990) Human arm stiffness characteristics during the maintenance of posture. Exp Brain Res 82:315–326

Franklin DW, Burdet E, Osu R, Kawato M, Milner TE (2003) Functional significance of stiffness in adaptation of multijoint arm movements in stable and unstable environments. Exp Brain Res 151:145–157

Gomi H, Kawato M (1997) Human arm stiffness and equilibrium-point trajectory during multi-joint movement. Biol Cybern 76:163–171

Gomi H, Osu R (1998) Task-dependent viscoelasticity of human multijoint arm and its spatial characteristics for interaction with environments. J Neurosci 18:8965–8978

Hogan N (1985) The mechanics of multi-joint posture and movement control. Biol Cybern 52:315–331

Hunter IW, Kearney RE (1982) Dynamics of human ankle stiffness: variation with mean ankle torque. J Biomech 15:747–752

Lacquaniti F, Carrozzo M, Borghese NA (1993) Time-varying mechanical behavior of multijointed arm in man. J Neurophysiol 69:1443–1464

McIntyre J, Mussa-Ivaldi FA, Bizzi E (1996) The control of stable postures in the multijoint arm. Exp Brain Res 110:248–264

Milner TE (2002a) Adaptation to destabilizing dynamics by means of muscle co-contraction. Exp Brain Res 143:515–519

Milner TE (2002b) Contribution of geometry and joint stiffness to mechanical stability of the human arm. Exp Brain Res 143:406–416

Mussa-Ivaldi FA, Hogan N, Bizzi E (1985) Neural, mechanical, and geometric factors subserving arm posture in humans. J Neurosci 5:2732–2743

Perreault EJ, Kirsch RF, Crago PE (2001) Effects of voluntary force generation on the elastic components of endpoint stiffness. Exp Brain Res 141:312–323

Perreault EJ, Kirsch RF, Crago PE (2002) Voluntary control of static endpoint stiffness during force regulation tasks. J Neurophysiol 87:2808–2816

Prochazka A, Trend PSJ (1988) Instability in human forearm movements studied with feedback-controlled muscle vibration. J Physiol (Lond) 402:421–442

Smeets JB, Erkelens CJ (1991) Dependence of autogenic and heterogenic stretch reflexes on pre-load activity in the human arm. J Physiol 440:455–465

Stein RB, Kearney RE (1995) Nonlinear behavior of muscle reflexes at the human ankle joint. J Neurophysiol 73:65–72

Tsuji T, Morasso PG, Goto K, Ito K (1995) Human hand impedance characteristics during maintained posture. Biol Cybern 72:475–485